ACADEMIC PRESS

Available online at www.sciencedirect.com

SCIENCE DIRECT®

Journal of Solid State Chemistry 177 (2004) 372–376

JOURNAL OF SOLID STATE CHEMISTRY

http://elsevier.com/locate/jssc

Structural difference between a superconducting sodium cobalt oxide and its related phase

Kazunori Takada,[a,c,*] Hiroya Sakurai,[b] Eiji Takayama-Muromachi,[b] Fujio Izumi,[a] Ruben A. Dilanian,[a] and Takayoshi Sasaki[a,c]

[a] *Advanced Materials Laboratory, National Institute for Materials Science, 1-1 Namiki, Tsukuba, Ibaraki 305-0044, Japan*
[b] *Superconducting Materials Center, National Institute for Materials Science, 1-1 Namiki, Tsukuba, Ibaraki 305-0044, Japan*
[c] *CREST, Japan Science and Technology Corporation, Japan*

Received 2 April 2003; received in revised form 3 June 2003; accepted 6 June 2003

Abstract

Monolayer hydrate (MLH) $Na_xCoO_2 \cdot y'H_2O$ was obtained from superconducting bilayer hydrate (BLH) $Na_xCoO_2 \cdot yH_2O$ by partial extraction of H_2O molecules between the CoO_2 layers. Magnetization measurements indicated that electron densities in the CoO_2 layer of the MLH phase remained unchanged after the water extraction. Nevertheless, superconductivity was completely suppressed in the MLH phase. This strongly suggests that the highly 2D nature in the BLH phase due to its thick insulating layers consisting of H_2O molecules and Na^+ ions plays an important role for inducing superconductivity.
© 2003 Elsevier Inc. All rights reserved.

Keywords: Superconductivity; Layered material; Hydrous sodium cobalt oxide

1. Introduction

Alkali-metal cobalt oxides with layered structure (A_xCoO_2) have attracted much interest not only in the physical aspect of their two-dimensional (2D) nature with triangular Co sublattice but also in their potential for practical applications. Li_xCoO_2 has already been used as a cathode material [1] in commercialized lithium-ion batteries, and $Na_{0.5}CoO_2$ shows large thermoelectric power [2]. Electric and magnetic properties have also been measured intensively in response to this interest, and a large amount of data has been presented for Na_xCoO_2 [2–6] and Li_xCoO_2 [7–11]. In spite of such extensive research, superconductivity has never been reported for this series of phases. Very recently, we discovered superconductivity in a layered sodium cobalt oxide, $Na_xCoO_2 \cdot yH_2O$ ($x \approx 0.35$, $y \approx 1.3$) [12].

Na_xCoO_2 consists of CoO_2 layers and charge-balancing Na^+ ions residing in the "galleries" between them [13]. The superconducting sodium cobalt oxide was evolved via soft-chemical modification of the layered structure of the parent oxide, $Na_{0.7}CoO_2$. We extracted a portion of Na^+ ions and inserted H_2O molecules in the galleries. The inserted H_2O molecules separated the CoO_2 layers far apart, resulting in a highly 2D nature in structure. The resultant sodium cobalt oxide showed superconductivity with a transition temperature (T_c) of ca. 5 K.

At this point, it is of primary importance to clarify the differences between our superconducting cobalt oxide and the many other non-superconducting phases with similar layered structures.

In the present study, we prepared a new hydrated sodium cobalt oxide with the same x-value, i.e., the same electron density, but with a different interlayer distance. We expected that studies on this material would be valuable for separating the effects of interlayer distance and electron density on superconductivity. Water molecules were extracted from the galleries to obtain such a layered oxide. In many layered host systems, discrete hydration states involving a monolayer or bilayer of H_2O molecules have been discovered [14]. Through similar topotactic reaction, H_2O molecules were extracted from the galleries, and a new sodium cobalt oxide, i.e., monolayer hydrate (MLH) $Na_xCoO_2 \cdot y'H_2O$, was obtained from the superconducting bilayer hydrate (BLH) $Na_xCoO_2 \cdot yH_2O$.

*Corresponding author. Fax: +81-29-854-9061.
E-mail address: takada.kazunori@nims.go.jp (K. Takada).

0022-4596/$ - see front matter © 2003 Elsevier Inc. All rights reserved.
doi:10.1016/S0022-4596(03)00336-0

2. Experimental method

BLH-$Na_xCoO_2 \cdot yH_2O$ was synthesized from the parent oxide, $Na_{0.7}CoO_2$, as described previously [12]. The MLH-$Na_xCoO_2 \cdot y'H_2O$ sample was obtained by storing BLH-$Na_xCoO_2 \cdot yH_2O$ under an N_2 gas flow for 6 days. Contents of Na and Co in the resulting sample were determined by inductively coupled plasma atomic-emission spectrometry (ICP-AES). The water content was calculated on the basis of the chemical formula, $Na_xCoO_2 \cdot y'H_2O$, using the Na and Co contents by ICP-AES.

Structural changes of BLH-$Na_xCoO_2 \cdot yH_2O$ under various relative humidities (RHs) were studied using an X-ray powder diffractometer (RINT 2100S, Rigaku) equipped with a sample chamber, in which RH is controlled. Cu$K\alpha$ radiation was used for the measurement. When it was necessary, the sample was put in a sample holder with an Al window to avoid exposure to ambient atmosphere.

Structure parameters of MLH-$Na_xCoO_2 \cdot y'H_2O$ were refined by the Rietveld method with the aid of a maximum-entropy method (MEM) using computer programs, RIETAN-2000 [15] and PRIMA [16], respectively. In the Rietveld refinement, based on space group $P6_3/mmc$ [17], preferred orientation was corrected with the March–Dollase function on the assumption of a (001) cleavage plane. In MLH-$Na_xCoO_2 \cdot y'H_2O$, the guest Na^+ ions and H_2O molecules are expected to be highly disordered, and MEM is quite effective for detailed analysis of such an intercalation compound. In MEM analysis, crystal structures are expressed not by structure parameters such as fractional coordinates and atomic displacement parameters but by electron densities in the unit cell. Consequently, MEM allows us to represent the disordered atomic configuration in a more appropriate way than in the conventional Rietveld analysis that adopts a split-atom model.

The magnetizations of the samples were measured by a superconducting quantum interference device (SQUID) magnetometer (MPMS 2SP, Quantum Design). The measurements were carried out under an external magnetic field of $H = 20$ Oe in a temperature range from 2 to 300 K by zero-field cooling (zfc) process.

3. Results and discussion

Fig. 1 shows the XRD patterns of BLH-$Na_xCoO_2 \cdot yH_2O$ under various RHs. Decreasing RH to 7% broadened the diffraction profiles of the original phase without significant shifts of the peak positions and produced new reflections at $d = 6.9$ and 3.4 Å ($2\theta = 12.8°$ and 25.8°, respectively). When the RH was increased from 7% to 90%, the intensities of these reflections decreased, and the reflections corresponding to the original phase were recovered. After the sample had been kept at an RH of 90% for 20 h, the additional reflections almost disappeared. Since only RH was changed during the procedure, the reaction was limited to either insertion or extraction of H_2O molecules with the H_2O content varying depending on RH. Finally, we found that the BLH phase disappeared completely after drying under an N_2 gas flow, forming a new phase, i.e., the MLH phase.

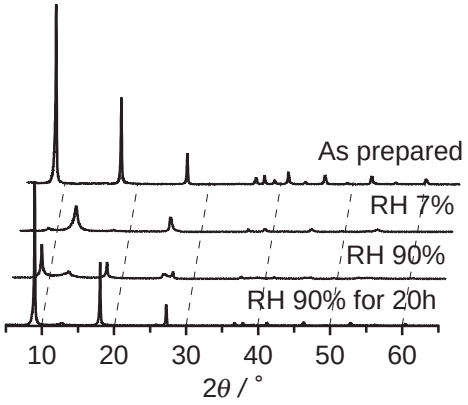

Fig. 1. XRD patterns of BLH-$Na_xCoO_2 \cdot yH_2O$ under various RHs.

The strongest reflections of 002 are located at $d =$ 5.5, 6.9, and 9.8 Å for the parent anhydrous $Na_{0.7}CoO_2$, MLH-$Na_xCoO_2 \cdot y'H_2O$, and BLH-$Na_xCoO_2 \cdot yH_2O$, respectively. This series of d values is similar to that observed in birnessites, MnO_2, an analog of the present system; anhydrous, monolayer hydrate, and bilayer hydrate birnessites have interlayer distances of 4.7–6, 7, and 10 Å, respectively [18]. The MLH-$Na_xCoO_2 \cdot y'H_2O$ has an interlayer distance similar to that in the monolayer hydrate birnessite, and thus its structure was refined on the basis of a monolayer hydration model.

Table 1 lists final structure parameters, and Fig. 2 shows Rietveld refinement patterns. The structure of MLH-$Na_xCoO_2 \cdot y'H_2O$ has a layer-stacking sequence similar to that in the parent phase or in BLH-$Na_xCoO_2 \cdot yH_2O$. It was rather difficult to differentiate Na^+ ions from H_2O molecules in the refinement because of pronounced static disorder of the guests. In the present structural model, Na^+ ions were located in 2c sites, and only fractional coordinates and occupancies of H_2O molecules were refined. The reason for adopting this arrangement will be discussed later. We also refined the structure starting from different models on the distributions of Na^+ ions and H_2O molecules, for example, without distinguishing Na^+ ions from H_2O molecules. However, MEM analysis afforded similar electron-density distribution independent of starting models; that is, high electron densities were always observed around the 2c sites. Fig. 3 shows representative electron-density

Table 1
Fractional coordinates, occupancies, g, and isotropic atomic displacement parameters, U, of MLH-$Na_xCoO_2 \cdot y'H_2O$

Atom	Site	x	y	z	g	U (Å^2)
Co	2*a*	0	0	0	1	0.0119(15)
O	4*f*	1/3	2/3	0.0666(5)	1	0.013(2)
Na	2*c*	1/3	2/3	1/4	0.358[a]	0.030(6)
WO[b]	6*h*	0.175(4)	$= 2x$(WO)	1/4	0.214(4)	$= U$(Na)

Space group: $P6_3/mmc$; $a = 2.8344(7)$ Å and $c = 13.842(5)$ Å; $R_{wp} = 9.40\%$ ($S = 2.04$), $R_p = 6.85\%$, $R_B = 1.29\%$, and $R_F = 2.73\%$.
[a] The total Na content x was fixed at 0.358, which was determined by ICP-AES.
[b] WO denotes an H_2O molecule, whose atomic scattering factor was set equal to the sum of one O and two H atoms.

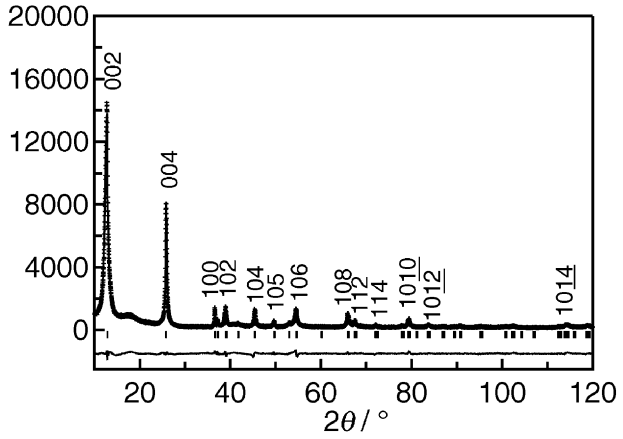

Fig. 2. Rietveld refinement patterns for MLH-$Na_xCoO_2 \cdot y'H_2O$. The observed diffraction intensities are represented by plus (+) marks, and the calculated pattern by a solid line. The curve at the bottom represents the weighted difference plots, $(Y_{io} - Y_{ic})/\sigma$, where Y_{io}, Y_{ic}, and σ are the observed and calculated intensities and the statistical uncertainty of the ith point, respectively. The differences were multiplied by 20 to make the plots easier to read. The short vertical bars below the observed and calculated patterns indicate the positions of allowed Bragg reflections. Only Miller indices for strong reflections are labeled.

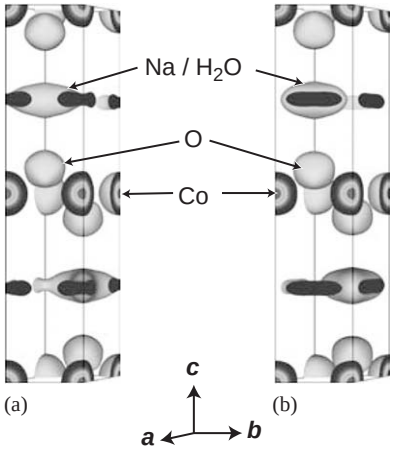

Fig. 3. Isosurfaces of electron densities determined for MLH-$Na_xCoO_2 \cdot y'H_2O$ by MEM. Equidensity level: 1.0/Å^3.

images resulting from two MEM analyses: Fig. 3a was obtained from the 'observed' structure factors, F_0, estimated on the basis of the result of the Rietveld

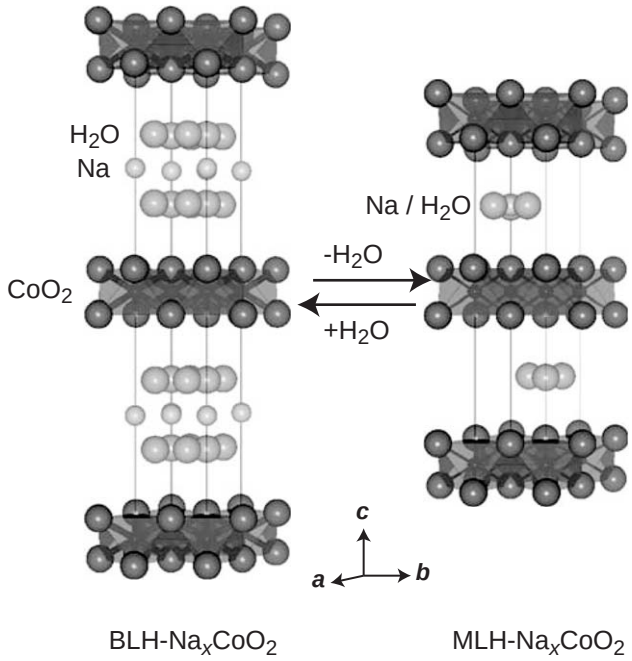

Fig. 4. Structural drawings of BLH-$Na_xCoO_2 \cdot yH_2O$ (left) and MLH-$Na_xCoO_2 \cdot y'H_2O$ (right), where Na and H_2O sites are partially occupied.

analysis using the present structural model and Fig. 3b was obtained using another structural model without differentiating Na^+ ions from H_2O molecules. From these findings, we concluded that the Na^+ ions reside around the 2*c* sites. To the best of our knowledge, this is the first case in which atomic positions are refined satisfactorily for a layered structure with highly disordered atoms such as in the present system. The resulting H_2O content was 0.64 per formula unit, which is quite consistent with the composition of $Na_{0.36}CoO_2 \cdot 0.70H_2O$ determined by ICP-AES. In addition, the final R factors were low enough to support our structural model.

Fig. 4 presents structural drawings of BLH-$Na_xCoO_2 \cdot yH_2O$ and MLH-$Na_xCoO_2 \cdot y'H_2O$ where the structure parameters of the BLH phase were cited from the previous report [12]. These structures are very similar to each other except for the contents and arrangements of Na^+ ions and H_2O molecules in the

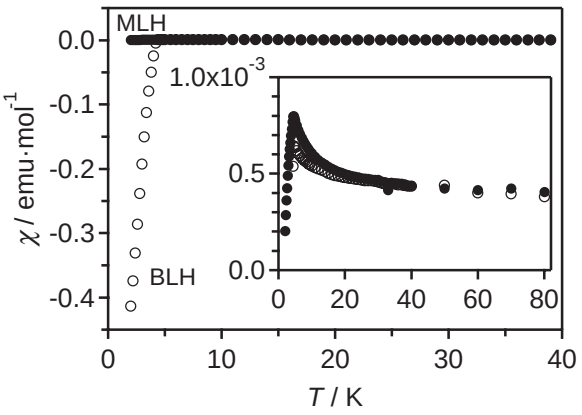

Fig. 5. Magnetic susceptibility (χ) of BLH-$Na_xCoO_2 \cdot yH_2O$ and MLH-$Na_xCoO_2 \cdot y'H_2O$. Closed and open circles indicate χ of BLH-$Na_xCoO_2 \cdot yH_2O$ and MLH-$Na_xCoO_2 \cdot y'H_2O$, respectively. The inset figure is an enlarged portion of positive χ.

galleries, which leads to a significant change in lattice parameter c.

Fig. 5 shows the magnetic susceptibilities (χ) of the samples measured under the zfc condition, where the vertical axis indicates a molar susceptibility. BLH-$Na_xCoO_2 \cdot yH_2O$ showed superconductivity with T_c of 5 K. Although MLH-$Na_xCoO_2 \cdot y'H_2O$ also showed a decrease of χ at the same onset temperature, the decrease was quite small and χ did not reach a negative value even at 2 K. As clearly seen in the figure, only BLH-$Na_xCoO_2 \cdot yH_2O$ showed bulk superconductivity. The decrease of χ observed for MLH-Na_xCoO_2 was considered to come from the residual phase of BLH-$Na_xCoO_2 \cdot yH_2O$, because the onset temperature did not change at all and the superconducting volume fraction was minimal. Indeed, the decrease of χ, i.e., $\chi(5\,K)$-$\chi(2\,K)$, for MLH-$Na_xCoO_2 \cdot y'H_2O$ was 5.7×10^{-4} emu mol^{-1}, which was 0.14% of 0.41 emu mol^{-1} for BLH-$Na_xCoO_2 \cdot yH_2O$. Thus, the decrease of χ can be explained if the MLH-$Na_xCoO_2 \cdot y'H_2O$ sample contained 0.14% BLH-$Na_xCoO_2 \cdot yH_2O$, and it is reasonable that such a small amount of BLH-$Na_xCoO_2 \cdot yH_2O$ would not be detected in the XRD pattern in Fig. 2.

The partial extraction of H_2O molecules from BLH-$Na_xCoO_2 \cdot yH_2O$ does not change the formal valence of cobalt, or the electron density in the CoO_2 layers. The reversible transformation between the BLH and MLH phases shown in Fig. 1 suggests that only the content of H_2O molecules changed without any other reactions such as oxidation or reduction during the formation of MLH-$Na_xCoO_2 \cdot y'H_2O$.

When the electron density in the CoO_2 plane changes, normal-state magnetic susceptibility should change significantly according to Kikkawa et al. [3]. They chemically extracted Na^+ ions from $NaCoO_2$ using iodine and measured their magnetizations. The extraction of Na^+ ions is accompanied by the change in the electron density of the CoO_2 layers, i.e., the extraction of electrons from the filled t_{2g} band. The measured χ at 20 K for Na_xCoO_2 with $x = 1.0$, 0.6, and 0.5 were 8.4×10^{-5} emu mol^{-1}, 6.2×10^{-4} emu mol^{-1}, and 4.3×10^{-4} emu mol^{-1}, respectively. On the contrary, the present samples had quite similar χ values above 20 K as shown in the inset of Fig. 5. These results give further evidence of the carrier density remaining unchanged.

The above consideration strongly suggests that adequate separation of the CoO_2 layers by the thick insulating layer of Na^+ ions and H_2O molecules is indispensable for superconductivity. As a matter of course, this does not mean that the electron (carrier) density is an immaterial parameter. Both factors are presumably important for superconductivity, but it can be concluded that the optimum level of carrier doping alone does not induce superconductivity.

Although the structures of CoO_2 layers in the present two compounds were almost identical, a slight difference in Co–O bond distance or distortion of CoO_6 octahedra may cause differences in band structure and may explain the appearance and disappearance of superconductivity. However, further discussion on such details is beyond the accuracy of the present structural refinement based on powder X-ray diffraction. Neutron diffraction is necessary for further discussion on the detailed structural differences between the CoO_2 layers of the phases.

The structure of MLH-$Na_xCoO_2 \cdot y'H_2O$ is worth further consideration, because it is a newly discovered phase. Sodium cobalt oxides that have been previously reported, e.g., $Na_{0.74}CoO_2$ [17] and β-$Na_{0.67}CoO_2$ [6], have interlayer distances of ca. 5.5 Å. A remarkable difference between the structures of MLH-$Na_xCoO_2 \cdot y'H_2O$ and these phases is in the atomic position of sodium in the galleries. The Na^+ ions in $Na_{0.74}CoO_2$ or β-$Na_{0.67}CoO_2$ reside almost at the centers of the trigonal prisms formed by the oxygen atoms, whereas in MLH-$Na_xCoO_2 \cdot y'H_2O$ they reside at the midpoints of the prism edges, i.e., at the midpoints between facing oxygen atoms of adjacent CoO_2 layers. Such a difference is considered to come from the different interlayer distances between the CoO_2 layers.

An attractive force would work in Na_xCoO_2 between its negatively charged CoO_2 layer and positively charged Na layer to reduce the interlayer distance. The interlayer distance of ca. 5.5 Å in $Na_{0.74}CoO_2$ or β-$Na_{0.67}CoO_2$ seems to be governed by the ionic radii of O^{2-} and Na^+ ions. Indeed, the interatomic distance between O and Na in the prism is equal to the sum of the ionic radii of O^{2-} (1.4 Å) and Na^+ (1.0 Å) [19]. On the contrary, the interlayer distance is 6.9 Å in the present MLH-$Na_xCoO_2 \cdot yH_2O$, because its CoO_2 layers are pillared not by Na^+ ions but by larger H_2O molecules. In this situation, the interatomic distance between facing oxygen atoms of adjacent CoO_2 layers is 5.1 Å, which is more than twice the sum of the ionic radii of Na^+ and

O^{2-} ions. This large distance causes the Na^+ ions to occupy the different sites from the center of the prism. Thus, the Na^+ ions occupy the 2*c* sites in MLH-$Na_xCoO_2 \cdot y'H_2O$, due to the strong attraction between the O^{2-} ion and the Na^+ ion. The Na^+ ion at the 2*c* site is coordinated by two oxygen atoms of the CoO_2 layers and, in addition, several H_2O molecules in the gallery, although the strongly disordered arrangement of the guests makes it difficult to determine the exact coordination geometry.

References

[1] K. Mizushima, P.C. Jones, P.J. Wiseman, J.B. Goodenough, Mater. Res. Bull. 15 (1980) 783–789.
[2] I. Terasaki, Y. Sasago, K. Uchinokura, Phys. Rev. B 56 (1997) R12685–R12687.
[3] S. Kikkawa, S. Miyazaki, M. Koizumi, J. Solid State Chem. 62 (1986) 35–39.
[4] T. Tanaka, S. Nakamura, S. Iida, Jpn. J. Appl. Phys. 33 (1997) L581–L582.
[5] T. Takeuchi, M. Matoba, T. Aharen, M. Ito, Physica B 312–313 (2002) 719–720.
[6] Y. Ono, R. Ishikawa, Y. Miyazaki, Y. Ishii, Y. Morii, T. Kajitani, J. Solid State Chem. 166 (2002) 177–181.
[7] W.D. Johnston, R.R. Heikes, D. Sestrich, J. Phys. Chem. Solids 7 (1958) 1–13.
[8] B. Buffat, G. Demazeau, M. Pouchard, J.M. Dance, P. Hagenmuller, J. Solid State Chem. 50 (1983) 33–40.
[9] I. Tomeno, M. Oguchi, J. Phys. Soc. Jpn. 67 (1998) 318–322.
[10] D. Carlier, I. Saadoune, L. Croguennec, M. Ménétrier, E. Suard, C. Delmas, Solid State Ionics 144 (2001) 263–276.
[11] S. Levasseur, M. Ménétrier, Y. Shao-Horn, L. Gautier, A. Audemer, G. Demazeau, A. Largeteau, C. Delmas, Chem. Mater. 15 (2003) 348–354.
[12] K. Takada, H. Sakurai, E. Takayama-Muromachi, F. Izumi, R.A. Dilanian, T. Sasaki, Nature 422 (2003) 53–55.
[13] C. Fouassier, G. Matejka, J.-M. Reau, P. Hagenmuller, J. Solid State Chem. 6 (1973) 532–537.
[14] R. Schöllhorn, in: M.S. Whittingham, A.J. Jacobson (Eds.), Intercalation Chemistry, Academic Press, New York, 1982 (Chapter 10).
[15] F. Izumi, T. Ikeda, Mater. Sci. Forum 321–324 (2000) 198–204.
[16] F. Izumi, R.A. Dilanian, in: Resent Research Developments in Physics, Vol. 3, Part II, Transworld Research Network, Trivandrum, 2003, in press.
[17] R.J. Balsys, R.L. Davis, Solid State Ionics 93 (1996) 279–282.
[18] R. Chen, P. Zavalij, M.S. Whittingham, Chem. Mater. 8 (1996) 1275–1280.
[19] R.D. Shannon, Acta Crystallogr. A 32 (1976) 751–767.